

Effective ATI channels in high harmonic generation

M. Yu. Kuchiev and V. N. Ostrovsky*

School of Physics, University of New South Wales, Sydney 2052, Australia

Abstract

Harmonic generation by an atom in a laser field is described by the three-step mechanism as proceeding via above-threshold ionization (ATI) followed by the electron propagation in the laser-dressed continuum and the subsequent laser assisted recombination (LAR). An amplitude of harmonic production is given by the coherent sum of contributions from different intermediate ATI channels labeled by the number m of absorbed laser photons. The range of m -values that gives substantial contribution is explored and found to be rather broad for high harmonic generation. The coherence effects are of crucial importance being responsible for the characteristic pattern of harmonic intensities with a *plateau* domain followed by a *cutoff* region. Due to multiphoton nature of the process, an efficient summation of m -contributions can be carried out in the framework of the saddle point method. The saddle points correspond to some complex-valued labels $m = m_c$ associated with the intermediate *effective ATI channels* in the three-step harmonic generation process. The advantage of this approach stems from the fact that summation over large number of conventional ATI m -channels is replaced by summation over small number of effective m_c -channels. The equation governing m_c has a transparent physical meaning: the electron ejected from the atom on the first (ATI) stage should return to the core to make LAR possible. The effective channel labels m move along characteristic trajectories in the complex plane as the system parameters vary. In the cutoff region of the harmonic spectrum a single effective channel contributes. For lower harmonics, in the plateau domain, two effective ATI channels become essential. The interference of their contributions leads to oscillatory pattern in the harmonic generation rates. The calculated rates are in good agreement with the results obtained by other approaches.

PACS numbers: 32.80.-t, 42.65.Ky, 32.80.Rm, 32.80.Wr

I. INTRODUCTION

A. Three-step mechanism of HHG

High efficiency of various processes in strong laser field could be understood basing on the observation that the field-induced *quiver motion* supplies an electron with high instantaneous energy. Rescattering of the energetic electron on atomic core generally is accompanied by the energy exchange between electron, core and electromagnetic field. In particular, the core could be excited or ionized [double ionization (DI) of an atom] and the high-energy photons could be emitted. The latter process is known as the harmonic generation (HG). If one considers the active electron initially bound to the core, then the electron at first should be (virtually) released to the quasi-free state, as a precondition that the subsequent events listed above become possible. As a whole, this constitutes *three-step mechanism* comprising above-threshold ionization (ATI), propagation in laser-dressed continuum and the final step which is electron-atom impact in case of rescattering, core excitation or ionization, or laser assisted recombination (LAR) in case of HG process. Strong interaction between the receding electron and the core is omitted in the standard Keldysh [1] model of multiphoton ionization. Its importance was first pointed out by Kuchiev [2], who had predicted several phenomena where the electron-core interaction plays a crucial role. The related mechanism was named “*atomic antenna*” to stress the role of active electron in gaining energy from laser field.

Specifically for HG the three-step model was promoted in the hybrid classical-quantum framework by Corkum [3], see also the papers by Kulander *et al* [4,5]. The subsequent theoretical developments were based on more sophisticated approaches and led to important advancements [6–11], albeit the three-step nature of the HG process was somewhat veiled in these formulations. Most clearly the three-step mechanism is exposed in the framework of *factorization* method developed in Ref. [12,13] as an implementation of idea of atomic antenna of Ref. [2] and applied to DI process. This technique allows one to present quantum amplitude as a direct sum over contributions of intermediate ATI channels. The application to HG process worked out by Kuchiev and Ostrovsky [14,15] quantitatively demonstrated validity and power of this approach. Since this development is the starting point of the present study, we briefly summarize it in Sec. IB below.

The intermediate ATI channels form a discrete set being labeled by a number m of absorbed photons. Generally speaking, entire manifold of m -channels contributes to the rate of three-step process under consideration. One can anticipate that actually only some effective m -range should be essential, but this issue has not been investigated previously. Another important question arises from the fact that contributions to the rate of three-step process from different ATI channels are to be summed coherently. How essential are *coherence effects* in reality remained unclear. The acuteness of this problem is enhanced in view of recent publications by Becker and Faisal [16–18] where semiempirical formula with *incoherent* summation is suggested in application to the DI process.

In the present paper we address these problems considering HG as the most simple three-step event. Being sharply important in itself, it hopefully provides a useful testground for other, more complicated processes. Our study shows that the range of efficiently contributing m -channels is rather broad (Sec. II). It is defined by interplay of two factors characterizing each m -channel contribution: the well known ATI amplitude (Appendix A) and much less

investigated LAR amplitude (Appendix B). Importantly, the phases of these amplitudes play a major role, showing that the coherence effects are crucial. In particular, solely these effects are responsible for the well-known rapid fall-off of HG rates beyond the so called *plateau* domain. At once this finding provokes a new question: how one can simplify summation over broad range of essential intermediate m -channels. We achieve this objective (Sec. III) by introducing a concept of *effective ATI channels*, or more briefly, effective channels (EC). Each EC is characterized by a complex-valued channel label m_c , i.e. a complex-valued number of absorbed photons. The latter is defined from the equation with simple and appealing physical meaning. The summation over a large number of intermediate m -channels is replaced by summation over very small number of EC (usually one or two). In the higher part of harmonic spectrum, beyond cutoff, it is sufficient to take into account a single EC. Two EC provide description of the plateau domain, including intricate oscillatory interference pattern of HG rates. As shown in Sec. IV, EC approximation ensures good quantitative agreement with the harmonic intensities obtained within other approaches [11,14,15].

As the system parameters vary, the EC labels m_c move along characteristic trajectories in the complex- m plane. This pattern condensedly expresses theoretical background of HG process in various regimes. For instance, transition between the regimes of one and two EC, i.e., between the cutoff and plateau domains, corresponds to “collision” of two trajectories in the complex plane. The oscillatory behaviour of HG rate in the plateau domain is explained by interference of two ECs. Thus ECs provide a unified framework for qualitative assessment of three-step processes as well as for their quantitative description. Probably the nearest analogy for this theoretical tool comprise the well-known Regge poles [19], i.e., the states with complex-valued angular momentum, that give an effective description in the quantum scattering theory.

B. Direct implementation of three-step mechanism in theory

Now it is worthwhile to look in more detail how the three-step mechanism of HG is implemented in the theory of Refs. [14,15]. The key formula for the amplitude of N -th harmonic generation,

$$d_N^+ = 2 \sum_m d_{Nm}^+ , \quad (1.1a)$$

$$d_{Nm}^+ = A_{m\mu_0}(\mathbf{K}_m) B_{Nm\mu_0}(\mathbf{K}_m) , \quad (1.1b)$$

presents it as a sum where each term is a product of two amplitudes of *physical, fully accomplished and observable* processes; no “off-shell” entities appear. The *first step* is described by the first factor $A_{m\mu_0}(\mathbf{K}_m)$ which is an amplitude of physical ATI process when after absorption of m laser photons the active electron acquires a translational momentum $\mathbf{p} = \mathbf{K}_m$; see detailed description of this amplitude within the Keldysh-type approach in Appendix A. The other factor, $B_{Nm\mu_0}(\mathbf{K}_m)$, is a combined amplitude of the *second and third steps*, i.e., propagation and laser assisted recombination (PLAR) amplitude. Under an additional approximation it can be factorized into propagation (expansion) factor $1/R_{m\mu_0}$ describing the *second step* and the amplitude of the *third step*, LAR, $C_{Nm}(\mathbf{K}_m)$:

$$B_{Nm\mu_0}(\mathbf{K}_m) = \frac{1}{R_{m\mu_0}} C_{Nm}(\mathbf{K}_m) . \quad (1.2)$$

$R_{m\mu_0}$ is merely an approximate expression for the distance passed by the active electron in course of its laser-induced wiggling motion, see Refs. [12,14,15] and formula (3.13c) below. The amplitude $C_{Nm}(\mathbf{K}_m)$ of the physical LAR process describes recombination, i.e., transition of electron with momentum \mathbf{K}_m from the continuum to bound state. Since the continuum state is laser-dressed, the recombining electron can emit the N -th harmonic photon, gaining necessary extra energy from the laser field. The formulas for LAR and PLAR amplitudes can be found in the Appendix B.

The summation in formula (1.1) runs over a number of photons m absorbed on the first step. Thus in the laser-dressed continuum the energy conservation constraint selects the discrete set of ATI channels, where the electron has a translational momentum \mathbf{K}_m . These channels serve as intermediate states for the three-step HG process. To specify exactly, the *absolute value* of the electron momentum in m -th ATI channel is defined by the energy conservation constraint in ATI as

$$K_m = \sqrt{2(m\omega - U_p + E_a)}. \quad (1.3)$$

where $E_a = -\frac{1}{2}\kappa^2$ is electron energy in the initial bound state, $U_p \equiv F^2/(4\omega^2)$ is the well-known ponderomotive potential, $\omega = 2\pi/T$ is the laser frequency, T is the period, \mathbf{F} is the electric vector in the linear-polarized laser wave. ATI can play role of the first stage of HG process only if the electron momentum has specific *direction*, namely \mathbf{K}_m is directed along \mathbf{F} . This ensures eventual electron return to the core that makes the final step, LAR, possible as discussed in detail in Refs. [12,14,15]. It is worthwhile to indicate once again that our approach presumes the single active electron approximation; the atomic units are used throughout the paper unless indicated otherwise. The observable HG rates \mathcal{R}_N are expressed via the amplitudes as

$$\mathcal{R}_N \equiv \frac{\omega^3 N^3}{2\pi c^3} |d_N^+|^2, \quad (1.4)$$

$\Omega = N\omega$ is the frequency of emitted harmonic, c is the velocity of light.

As already mentioned, the general framework for three-step decomposition of complicated laser-induced processes is provided by factorization technique of Ref. [12]. The accuracy of this theoretical device is governed by multiphoton nature of the processes: the larger is number of laser quanta involved, the more accurate results it provides. To avoid confusion, it should be emphasized that the factorization *is not* related to the conventional perturbation theory, or to its simplified version known as the pole approximation.

Here we only briefly outline some features of the derivation [12,14,15] necessary for understanding of the present development. The basic expression for the HG amplitudes contains integration over two time variables, t and t' . The factorization technique allowed us to disentangle these integrations basing on the adiabatic approach. Mathematically the latter implies the saddle point approximation for calculating the integrals which emerge when a particular representation for the Green function in terms of intermediate states is chosen. The saddle point integration over time variable t' is intrinsic for the factorization technique, whereas another time integration could be carried without approximations, for instance, numerically. The latter approach was adopted in Refs. [14,15] and in Sec. II of the present paper. However, EC approximation implies saddle point integration also over time variable t . The details could be found in Appendices A and B. Here we only indicate

physical meaning of the emerging saddle points. For t' variable the saddle point $t'_{m\mu_0}$, being given by Eq. (A7), is the instant of time when the electron is emitted into an intermediate ATI channel. The saddle point in t -integral, $t_{Nm\mu}$, see Eq. (B13), is the time of laser-assisted recombination of electron with the core, accompanied by emission of high-energy photon. Note that generally both $t'_{m\mu_0}$ and $t_{Nm\mu}$ are complex-valued.

Formula (1.1) is important conceptually being the most direct and fully quantum description of the three-step mechanism of HG. It can serve also as a practical computational tool. The latter statement was testified by a very good quantitative agreement between calculations of HG rates by formulae (1.1), (1.4) [14,15] and the benchmark results by Becker *et al* [11] for HG by H^- ion. However, as discussed in Sec. IA, it was not explored before what is the range of channel label m that gives substantial contribution to the rate. This problem is addressed in Sec. II where we show that a rather large number of intermediate ATI channels is to be taken into account. The effective summation method of Sec. III transforms sum (1.1a) over large number of m -terms to the sum over very small number (one or two) of EC terms. The illustrative applications of EC approach in Sec. IV serve to demonstrate its reliability. EC representation is convenient also for analysis of general features of HG spectrum. The latter is known to consist of three parts. The initial rapid decrease is followed by the *plateau* domain and the rapid *cutoff* region. Being interested in the generation of rather high harmonics, we do not consider below the initial low- N part of the spectrum. The upper boundary N_b of the plateau is given by the known expression [4,5,7,11]

$$N_b \omega = \frac{1}{2} \kappa^2 + 3.17 U_p . \quad (1.5)$$

In Sec. IIIC we show how this important result follows from the three-step mechanism cast in the EC form. Section V contains concluding discussion.

II. COMPOSITION OF HG AMPLITUDE FROM ATI CONTRIBUTIONS

Representation (1.1) of HG amplitudes d_N^+ as a sum over ATI contributions is characterized by a number of interesting features. We illustrate them by Fig. 1 where different terms in the sum (1.1a) are quantitatively presented for HG by H^- ion in the laser field with the frequency $\omega = 0.0043$ and the intensity $I = 10^{11}$ W/cm². We show separately the squared moduli and phases for the ATI amplitude $A_{m\mu_0}$ (open squares), PLAR amplitude $B_{Nm\mu_0}$ (open triangles) and the resulting term in the sum (1.1a) d_{Nm}^+ (closed circles) in dependence on m for some representative values of the harmonic order N . Namely, $N = 15, 25$ lie in the plateau domain of HG spectrum whereas $N = 39, 51$ are in the cutoff region. Only open intermediate ATI channels are included in summation (1.1a) that in the present case means $m \geq 16$.

The following observations could be made.

- The number of m -terms giving substantial contribution to the sum (1.1a) is essentially independent of N being about 15 in the example under consideration.
- The domain of m giving substantial contribution is defined, first, by the monotonous decrease of $|A_{m\mu_0}|^2$ with m that ensures effective cut-off from the high- m side. The

second factor $|B_{Nm\mu_0}|^2$ has more complicated behavior. Indeed, it oscillates with m and has substantial magnitude in the much broader range of m than $|A_{m\mu_0}|^2$ (this issue is discussed in more detail in the Appendix B). In HG process it is important that for high harmonic order N the factor $|B_{Nm\mu_0}|^2$ is strongly suppressed in the low- m region (i.e. near ATI threshold, see Figs. 1c,d). Therefore, as N increases, the domain of important contributions to the sum shifts to higher m .

- Typical values of the *modulus squared components* $|d_{Nm}^+|^2$ decrease with the harmonic order N increasing. This is explained by decrease in the typical values of the $|B_{Nm\mu_0}|^2$ factor (note that $|A_{m\mu_0}|^2$ does not depend on N). Importantly, this relatively slow decrease cannot explain the cutoff in the spectrum of *modulus squared amplitudes* $|d_N^+|^2$. For instance, as N varies from 39 to 51 the typical values of $|d_{Nm}^+|^2$ decrease only by a factor about 3, whereas the resulting $|d_N^+|^2 = |\sum_m d_{Nm}^+|^2$ decreases by seven orders of magnitude ! This clearly indicates that the high- N cutoff of HG rate is due to the strong *cancellation of terms* in the sum (1.1a), i.e. that the *coherence or phase effects* are crucial.
- The plots of the phases show that $\arg(A_{m\mu_0})$ decreases with m whereas $\arg(B_{Nm\mu_0})$ increases. The resulting phase $\arg(d_{Nm}^+) = \arg(A_{m\mu_0}) + \arg(B_{Nm\mu_0})$ grows with m rather rapidly. For larger N variation of phases becomes faster. For instance, in the case $N = 51$ the phase $\arg(d_{Nm}^+)$ increases by about 10π along the substantial m -domain ($20 < m < 35$). Namely the rapid phase variation governs cancellations in the sum (1.1a) and rapid decrease of the HG rates in the fall-off region.

The rapid variation of phases is generally characteristic for the semiclassical dynamics. Therefore one can suggest that in our problem some semiclassical-type method of summation over ATI contributions could be developed that reflects the physics of the process. This program is implemented in the next section.

III. EFFECTIVE ATI CHANNELS

A. Poisson summation of ATI channel contributions

Further in the basic formula (1.1) we employ for both ATI and PLAR amplitudes the saddle-point approximation given by formulas (A2) and (B9), respectively. This representation possesses important advantage of explicitly exposing large phases of amplitudes which are of crucial significance in coherent summation as revealed in previous section. The phase factors have form of exponents of classical action for the ATI and LAR processes. By using these expressions we present the HG amplitude (1.1) as

$$d_N^+ = 2 \sum_m \sum_\mu \mathcal{Q}_{m\mu} \exp \left[-i\mathcal{S} \left(t_{m\mu}, t'_{m\mu_0} \right) \right] . \quad (3.1)$$

Bearing in mind importance of phase factors we write down them explicitly in Eq. (3.1), introducing

$$\mathcal{S}(t, t') = S(t) - S(t') + \Omega t = \frac{1}{2} \int_{t'}^t d\tau \left[\left(\mathbf{K}_m + \frac{\mathbf{F}}{\omega} \sin \omega \tau \right)^2 - E_a \right] + \Omega t, \quad (3.2)$$

whereas all the rest is collected in the pre-exponential factor $\mathcal{Q}_{m\mu}$:

$$\begin{aligned} \mathcal{Q}_{m\mu} = & -\frac{\omega^4}{2\pi} A_a \Gamma(1 + \nu/2) 2^{\nu/2} \kappa^\nu Y_{lm_{az}}(\hat{\mathbf{p}}_{\mu_0}) \frac{1}{F(\cos \omega t'_{m\mu_0} - \cos \omega t_{m\mu})} \times \\ & \times \tilde{\phi}_a^{(\epsilon)} \left(-\mathbf{K}_m - \frac{\mathbf{F}}{\omega} \sin \omega t_{m\mu} \right) \frac{1}{\sqrt{S''(t'_{m\mu_0})^{\nu+1} S''(t_{m\mu})}}. \end{aligned} \quad (3.3)$$

$\mathcal{S}(t, t')$ has an appealing meaning of action for HG processes expressed as a sum of actions for constituent ATI and LAR processes.

From the pragmatic point of view the attractive feature of the sum representations (1.1) or (3.1) is obvious: each term in the sum has a clear and simple analytical expression, that helps greatly in numerical calculations. However, since the number of essential terms in the sum is large, as discussed in Sec. II, the behavior of the sum may differ drastically from behavior of its individual terms. This makes difficult an interpretation of the results which follow from (1.1) or (3.1). To overcome this disadvantage it is highly desirable to find some other representation for the amplitude which would be devoid of extended summations. One can obtain guideline for practical implementation of this idea by recalling the fact that summation in (1.1) or (3.1) runs over the *spectrum* of intermediate ATI states. From the general physical principles we know that when the spectrum covers a broad range of energies it could be advantageous to work within the time-dependent picture. Mathematically this implies the Fourier transformation which replaces the spectral quantities $m\omega$ with appropriate intervals of time.

Having these arguments in mind, we carry out the Poisson summation in (3.1) that could be looked at as desired ‘‘Fourier transformation’’

$$d_N^+ = 2 \sum_{j=-\infty}^{\infty} \int_{-\infty}^{\infty} dm \sum_{\mu} \mathcal{Q}_{m\mu} \exp \left[-i\mathcal{S}(t_{m\mu}, t'_{m\mu_0}) - 2\pi i j m \right]. \quad (3.4)$$

Transition from (3.1) to (3.4) amounts to replacing summation over the integer m by integration over related continuous variable. The price is introducing an extra (and infinite) summation over an integer j . The transformation is worthy if the latter sum effectively contains less terms than the original m -sum (1.1a), i.e., converges more rapidly.

B. Saddle point method and effective channel representation

Our next step is evaluation of integrals over m in (3.4). As demonstrated in Sec. II, the phase of the term d_{Nm}^+ in the sum (1.1a) varies rapidly with the summation index m . Physically this follows from a multiphoton nature of the process under consideration. We presume that the exponent in (3.4) is responsible for this, whereas the pre-exponential factor $\mathcal{Q}_{m\mu}$ varies slowly. This allows us to use the saddle point method to carry out explicitly the integration over the ATI channel label m . The position of the saddle point(s) is governed by equation

$$\frac{d}{dm} \mathcal{S}(t_{m\mu}, t'_{m\mu_0}) = -2\pi j . \quad (3.5)$$

When taking derivative in Eq. (3.5) one has to remember that there are two sources of m -dependence: first, via $t'_{m\mu_0}$ and $t_{m\mu}$ that are the integration limits in the definition (3.2), and, second, via K_m that enters the integrand in (3.2). However the situation is drastically simplified by the fact that

$$\left. \frac{\partial}{\partial t'} \mathcal{S}(t, t') \right|_{t'=t'_{m\mu_0}} = 0 , \quad (3.6a)$$

$$\left. \frac{\partial}{\partial t} \mathcal{S}(t, t') \right|_{t=t_{m\mu}} = 0 \quad (3.6b)$$

since $t'_{m\mu_0}$ and $t_{m\mu}$ are the saddle points in integration respectively over t' and t variables as discussed briefly in Sec. I and in more detail in Appendices A and B, see formulae (A5) and (B11). Therefore Eq. (3.5) takes a compact form ($dK_m/dm = \omega/K_m$)

$$\left[K_m (t - t' + jT) + \frac{F}{\omega} \int_{t'}^t \sin \omega \tau d\tau \right]_{t'=t'_{m\mu_0}; t=t_{m\mu}} = 0 , \quad (3.7a)$$

or, more explicitly,

$$K_m (t_{m\mu} - t'_{m\mu_0} + jT) = \frac{F}{\omega^2} (\cos \omega t_{m\mu} - \cos \omega t'_{m\mu_0}) . \quad (3.7b)$$

It is to be considered together with formulae (A7) and (B13) defining positions of saddle points in integration over t' and t variables respectively. The unknown variable to be defined is the ATI label $m_c(N, j)$. As shown below, only complex-valued solutions are possible. Note that m enters (3.7b), (A7) and (B13) only via K_m (1.3). Therefore solution of the saddle point equation (3.7b) amounts to finding complex-valued translational momentum $K_{m_c}(N, j)$ of electron in the intermediate ATI channel that gives major contribution to the generation of N -th harmonics.

Within the saddle point approximation formula (3.4) is reduced to

$$d_N^+ = 2 \sum_{j=-\infty}^{\infty} \sum_{m_c} \sum_{\mu} \mathcal{Q}_{m_c\mu} \sqrt{\frac{2\pi}{i\mathcal{S}''_{m_c}}} \exp \left[-i\mathcal{S}(t_{m_c\mu}, t'_{m_c\mu_0}) - 2\pi i j m_c \right] , \quad (3.8)$$

where

$$\begin{aligned} \mathcal{S}''_{m_c} \equiv \frac{d^2}{dm^2} \mathcal{S}(t_{m\mu}, t'_{m\mu_0}) \Big|_{m=m_c} &= \frac{\omega^2}{K_m^2} (t_{m_c\mu} - t'_{m_c\mu_0} + jT) + \\ &+ \frac{\omega}{K_{m_c}} \left(\sqrt{2N\omega - \kappa^2} \frac{dt_{m\mu}}{dm} - i\kappa \frac{dt'_{m\mu_0}}{dm} \right) \Big|_{m=m_c} . \end{aligned} \quad (3.9)$$

The necessary derivatives are straightforwardly derived using formulas (A7) and (B13), respectively, as

$$\frac{dt'_{m\mu_0}}{dm} = -\frac{\omega}{K_m F \cos \omega t'_{m_c\mu_0}}, \quad \frac{dt_{m\mu}}{dm} = -\frac{\omega}{K_m F \cos \omega t_{m_c\mu}}. \quad (3.10)$$

Even more appealing form of expression (3.8) is obtained if one reexpresses the constituent factors in terms of ATI and LAR amplitudes:

$$d_N^+ = 2 \sum_j \sum_{m_c} A_{m_c\mu_0}(\mathbf{K}_{m_c}) \frac{1}{R_{m_c\mu\mu_0}} C_{Nm_c}(\mathbf{K}_{m_c}) \Xi(m_c, j), \quad (3.11)$$

$$\Xi(m_c, j) \equiv \sqrt{\frac{2\pi}{i\mathcal{S}_{m_c}''}} \exp(-2\pi i j m_c). \quad (3.12)$$

Here we omit summation over μ implying that it is absorbed into the sum over m_c , since each saddle point m_c is obtained for some choice of label μ . The form of expansion (propagation) factor

$$\frac{1}{R_{m\mu\mu_0}} = \frac{\omega^2}{F (\cos \omega t_{m\mu} - \cos \omega t'_{m\mu_0})} \quad (3.13a)$$

is a natural specification of the more general expression obtained earlier [15,14] and cited in Eq. (B3). In particular, at the saddle point one can use Eq. (3.7b) to rewrite propagation factor as

$$\frac{1}{R_{m_c\mu\mu_0}} = \frac{1}{K_{m_c} (t_{m_c\mu} - t'_{m_c\mu_0} + jT)}. \quad (3.13b)$$

Formula (3.11) provides the most concentrated expression of the result of present work. Apart from the smooth factor $\Xi(m_c, j)$, it is fully analogous to our starting point expression (1.1), but with summation over large number of intermediate ATI channels m replaced in Eq. (3.11) by summation over small number of effective channels m_c . Note that the factorization of propagation and LAR amplitudes, as given by formula (1.2), appears as an additional approximation in the framework of our previous approach [14,15] where the t -integration was carried out numerically. In the EC formulation the factorization is a necessary feature, due to the saddle-point method applied to calculation of integral over time variable t , see Appendix B. The form (3.13a) of the expansion factor is more accurate than the approximation

$$\frac{1}{R_{m\mu_0}} = -\frac{\omega^2}{F \cos \omega t'_{m\mu_0}} \quad (3.13c)$$

discussed (within unessential sign) earlier [14,15] and implied in formula (1.2) of the present paper.

The transparent interpretation of the saddle point equation (3.7a) is based on the fact that

$$z(t, t'; p) = p(t - t' + jT) + \frac{F}{\omega} \int_{t'}^t \sin \omega \tau d\tau \quad (3.14)$$

is the electron displacement along z -axis in course of its wiggling motion in the laser field as time varies from t' to t . The axis is directed along the electric field vector \mathbf{F} ; the electron

translational momentum \mathbf{p} has the same direction. In terms of $z(t, t'; p)$ (3.14) the saddle point equation (3.7a) can be equivalently rewritten as

$$z(t_{m\mu} + jT, t'_{m\mu_0}; K_m) = 0. \quad (3.15)$$

This equation has a lucid physical meaning. In the semiclassical picture of HG, as implemented by the present theory, the electron emerges from the under barrier at the instant of time $t'_{m\mu_0}$ into the m -th channel of ATI continuum and undergoes backward transition into the bound state with emission of the Ω photon at time $t_{m\mu}$. Both these events occur relatively close to the atomic core. Eq. (3.15) is the condition that after propagation in the laser field the electron returns *exactly* [20] to the emission point. It accounts to the fact that the propagation time could be augmented by additional j laser field periods T . The integer parameter j conjugate to m in the ‘‘Fourier transformation’’ (3.4) can be named a *recursion number*. As discussed above, in fact equation (3.15) defines an appropriate electron momentum K_{m_c} . The latter proves to be complex-valued as shown below.

The return condition (3.15) is universal in the sense that it does not contain explicitly the harmonic order N (the latter parameter implicitly defines the return time $t_{m\mu}$). The condition of return is intrinsic in the physical picture of the three-step process. Being constituent part of the atomic antenna idea of Ref. [2], it appeared in some form in previous studies by other authors. The most close links could be established with Ref. [8]. This paper employs a different representation that does not appeal to the intermediate ATI channels. Nevertheless the saddle point method applied in these calculations also leads to the equation for the saddle points with the same physical meaning. Moreover, the same number of saddle points plays substantial role (namely, one point at the cutoff region and two points at the plateau domain, see below). Unfortunately the saddle point evolution with varying harmonic order N was not described in detail in the cited paper. Note also that the cited paper provides the HG rates only within an adjustable normalization factor.

As already mentioned, the summation over j in the formulas (3.4), (3.8) or (3.11) reflects the fact that the time interval between the emission of electron and emission of the high-energy photon could be different; namely, several (j) periods of the laser field could be added to it. All these events add up coherently as show Eqs. (3.8) or (3.11). The shortest time interval corresponds to $j = 0$. Physically one can anticipate that the related contribution prevails because of a spread of electron wave packet. Mathematically the term with $j = 0$ is obtained by plain replacement of the summation over m in Eq. (1.1) by integration. Further on we concentrate on calculation of this term and consider at first (Sec. III C) the related saddle points $m_c(N) \equiv m_c(N, j = 0)$.

Let us discuss now a restriction on the summation index j in (3.8). In the saddle point method one deforms the integration contour so that it passes via the saddle points; only close vicinities of the saddle point effectively govern the integral magnitude. Generally, the shifted contour passes only via some subset of the saddle points available; only the points from this subset contribute to the integral. We deal with multi-dimensional problem (integration over variables m, t, t') that casts analysis of the integration contour deformation as a complicated task. To circumvent this obstacle we adopt an approach based on simple physical arguments. As discussed above, the recursion number j counts a number of periods of time that elapse between the electron escape and its return to the atom. The three-step mechanism presumes that the moment of escape must precede the moment of return. This condition can only be

satisfied for non-negative values of j . Basing on this physical argument we assume that the saddle points m_c contribute to the integral only for non-negative $j \geq 0$.

Saddle points m_c which contribute to summation over m_c in formula (3.8) should satisfy additional condition

$$\text{Im} \left[\mathcal{S} \left(t_{m_c\mu}, t'_{m_c\mu_0} \right) + 2\pi j m_c \right] < 0, \quad (3.16)$$

which ensures that the factor in the exponent in the right-hand side of Eq. (3.8) always reduces the absolute value of the amplitude. Again we do not attempt to validate (3.16) mathematically, but note instead that this condition is very similar to a conventional restriction on the resonances in stationary processes. Remember that the energy E_0 of a conventional resonance has the real and imaginary parts. The later one describes the width of the resonance $\text{Im}E_0 = -\Gamma/2 < 0$, and must be negative. In the time-dependent formalism the resonance contribution to the amplitude is given by the factor $\exp(-iE_0t)$, where $t > 0$ is the time elapsed since the resonance intermediate state has been excited. The condition $\text{Im}E_0 < 0$ selects one of two complex-conjugate poles of the S -matrix, or Green function, thus ensuring the decay of the resonance, i.e., that $|\exp(-iE_0t)| < 0$. Similar physical meaning has Eq. (3.16).

Eqs. (3.8) or (3.11) are the major result of this paper. They implement the objective formulated in Sec. III A to carry out the ‘‘Fourier transformation’’ of Eq. (3.4). The latter expression includes summation over the physical, discrete spectrum m of the intermediate ATI states. In contrast, Eq. (3.8) refers to some complex-valued m_c which label EC. Additionally, Eq. (3.8) includes summation over recursion number j , that is a number of laser periods T that elapse between the ionization and HG generation. It is important that the sum over j converges well. The reason for this originates from the discussed above fact of the slow convergence of the spectral representation (3.4). It is a general, well known fact that if the spectral pattern is broad, then the ‘‘Fourier transformation’’ should be well localized. Same argument can be presented from another point of view. The shortest (positive) time interval between the ionization and HG emission corresponds to $j = 0$. One can anticipate that the related contribution prevails because the spread of the electron wave packet should significantly diminish contributions of events with larger j . Presuming that this argument is correct, we will replace in the applications (Sec. IV) summation over j in Eq. (3.11) by the only term with $j = 0$. Good numerical results obtained illustrate the fact that the term $j = 0$ really dominates. For $j = 0$ we find only few (one or two) operative EC m_c . Thus the sum (3.11) over EC comprises very few terms that is convenient for interpretation of the results.

The physical background of the mathematical transformations above can be briefly summarized as follows. The electron motion in a laser field in the vicinity of an atom satisfies the adiabatic condition because the number of laser quanta absorbed and emitted in the HG process is large. The HG amplitude contains a large phase that is identical to the classical action $\mathcal{S}(t, t')$ (3.2). This phase varies rapidly with all the parameters that govern the electron propagation in the intermediate state. Therefore the major contribution to the event comes from such situations in which the phase is stationary, i.e. from the saddle points. The phase depends on the initial moment of virtual ionization t' , the final moment of the harmonic emission t and the energy of the electron in the intermediate state. Eqs. (3.6a), (3.6b), (3.5) represent the saddle-point conditions over these three variables. Altogether

they define the two moments of time and the electron energy in the intermediate state.

C. Analysis of saddle point equation

By summing and subtracting Eqs.(A7) and (B13) we obtain

$$\sin \omega t_{m\mu} + \sin \omega t'_{m\mu_0} + 2K_m \frac{\omega}{F} = 2\mathcal{Z} , \quad (3.17a)$$

$$\sin \omega t_{m\mu} - \sin \omega t'_{m\mu_0} = 2\mathcal{Z}' , \quad (3.17b)$$

with

$$\mathcal{Z} \equiv \frac{1}{2} \left(\sqrt{2N\omega - \kappa^2} + i\kappa \right) \frac{\omega}{F} , \quad \mathcal{Z}' \equiv \frac{1}{2} \left(\sqrt{2N\omega - \kappa^2} - i\kappa \right) \frac{\omega}{F} . \quad (3.18)$$

If $2N\omega > \kappa^2$, then one has $\mathcal{Z}^* = \mathcal{Z}'$. It is convenient to switch from $t'_{m\mu_0}$ and $t_{m\mu}$ to

$$x = \frac{1}{2} \omega \left(t_{m\mu} + t'_{m\mu_0} \right) , \quad y = \frac{1}{2} \omega \left(t_{m\mu} - t'_{m\mu_0} \right) \quad (3.19)$$

and present (3.17a) and (3.17b) in the compact form

$$\sin x \cos y + K_m \frac{\omega}{F} = \mathcal{Z} , \quad (3.20a)$$

$$\cos x \sin y = \mathcal{Z}' . \quad (3.20b)$$

In the same notation Eq. (3.7b) reads

$$K_m \frac{\omega}{F} = -\frac{\sin x \sin y}{y + j\pi} . \quad (3.21)$$

By excluding K_m we obtain a set of two equations for two variables x and y :

$$\sin x \left(\cos y - \frac{\sin y}{y + j\pi} \right) = \mathcal{Z} , \quad (3.22a)$$

$$\cos x \sin y = \mathcal{Z}' . \quad (3.22b)$$

The next step is to exclude x that after some algebra gives a compact transcendental equation for a single variable $\tilde{y} = y + j\pi$:

$$\left(\cot \tilde{y} - \frac{1}{\tilde{y}} \right)^2 \left[\sin^2 \tilde{y} - (\mathcal{Z}')^2 \right] = \mathcal{Z}^2 . \quad (3.23)$$

As soon as \tilde{y} is found, one obtains K_m from

$$\frac{\omega}{F} K_m = \frac{\mathcal{Z}}{1 - \tilde{y} \cot \tilde{y}} . \quad (3.24)$$

The variable y (3.19) has a very lucid meaning: $2y/\omega$ is the active electron excursion time in the continuum, i.e., the time interval between the first step in the three-step process, ATI

and the last step, LAR. Change in the recursion number j is equivalent to change of the excursion time $(t_{m\mu} - t'_{m\mu_0})$ by an integer multiple of laser period T . To simplify subsequent analysis we restrict it to the case $j = 0$, or $0 \leq \tilde{y} = y < \pi$, that gives the major contribution to the amplitude, as discussed in Sec. III B.

When generation of high harmonics is considered, $2N\omega \gg \kappa^2$, the estimate

$$\sqrt{2N\omega - \kappa^2} \gg \kappa \quad (3.25)$$

is valid that implies that one can put $\mathcal{Z}' \approx \mathcal{Z} \approx \sqrt{2N\omega - \kappa^2} \omega / (2F)$. This allows us to rewrite equation (3.23) governing saddle point positions in an approximate form

$$f(y^2) = \frac{\omega^2}{4F^2} (2N\omega - \kappa^2) , \quad (3.26)$$

with the universal function $f(y^2)$ of a dimensionless parameter y defined as

$$f(y^2) \equiv \frac{(y \cot y - 1)^2 \sin^2 y}{(y \cot y - 1)^2 + y^2} . \quad (3.27)$$

A plot of this function (Fig. 2) shows that in the interval of interest, $0 \leq \xi = y^2 < \pi^2$ it has a single maximum located at $\xi_m = 4.173$ ($y_m = 2.043$). For sufficiently small N , when the right hand side of Eq. (3.26) is less than $C_1 \equiv f(\xi_m) = 0.3966$, this equation has two solutions designated as A and B in Fig. 2 where this situation is explicitly displayed. One can verify that these solutions satisfy condition (3.16) and therefore both of them contribute to the HG amplitude. Note that both solutions correspond to real but different excursion times $2y/\omega$.

When N increases, the roots A and B come closer and eventually merge at some critical value of $N = N_b$ defined from

$$\frac{\omega^2}{4F^2} (2N_b \omega - \kappa^2) = C_1 , \quad (3.28)$$

that is

$$N_b \omega = \frac{1}{2} \kappa^2 + C_1 \frac{2F^2}{\omega^2} = \frac{1}{2} \kappa^2 + 3.1731 U_p . \quad (3.29)$$

For larger $N > N_b$ the solutions A and B split again, but this time they result in complex-valued y . The way to see this, is to note that in the vicinity of the maximum the function $f(y^2)$ behaves as $f(y^2) - f(y_m^2) \sim -(y - y_m)^2$. Further straightforward analyses indicates that only one of these two complex-valued solutions satisfies condition (3.16) and contributes to the amplitude, while another one gives no contribution.

Thus the number and the character of relevant solutions of Eq. (3.26) differs for $N < N_b$ and $N > N_b$. The excursion time switches from real to complex-valued that indicates that the HG process changes its nature from the classically allowed to classically forbidden one. Accordingly, as detailed in Sec. IV, at the point $N < N_b$ the HG spectrum undergoes a transition from the plateau to the cutoff region. Thus Eq. (3.29) rederives the well-known upper border of the plateau domain in the HG spectrum (1.5) with a slightly different

coefficient in front of U_p . The validity condition for this derivation (3.25) essentially means that the photon energy $N_b\omega$ is much higher than the initial electron binding energy $\frac{1}{2}\kappa^2$.

Before concluding this subsection we remark that one more solution of Eq. (3.26) is shown in Fig. 2, being labeled as C. It corresponds to negative y^2 and has simple N -dependence since the function $f(y^2)$ is monotonous on the semiaxis $y^2 < 0$. The fact that the solution C results in imaginary excursion time $2y/\omega$ indicates that it gives small contribution to the HG amplitude.

IV. ILLUSTRATIVE APPLICATIONS

A. Scanning harmonic order for fixed laser intensity

There are two natural and complementary outlooks on the results for HG process. One can fix the laser intensity I and scan the rates for harmonics of different order, as done in this subsection, or one can fix the harmonic order N and vary the laser intensity (Sec. IV B). In both cases we consider HG by H^- ion in the laser field with the frequency $\omega = 0.0043$.

Fig. 3 depicts a typical pattern of evolution of $m_c(N)$ in the complex- m plane for fixed laser field intensity $I = 10^{11}$ W/cm². Positions of three complex-valued roots of the exact saddle-point equation (3.7b) are shown by symbols of different shape. The roots move as the harmonic order N varies; we show their positions for odd (physical) values of N . For large N only one root has negative imaginary part (it is shown by diamonds in Fig. 3) that ensures harmonic rate decrease with increasing N . Fig. 4 shows results of the rates calculation in the saddle point approximation (3.8) where only this single root is taken into account in the summation over m_c . The cutoff region in the rates spectrum is nicely reproduced, as well as the overall pattern in the plateau domain. However the single-saddle-point approximation does not reproduce some structures in the N -dependence of HG rates. In the plateau domain the saddle point $m_c(N)$ moves close to the real m -axis. For small N this saddle point approaches the point $m = m_{\text{th}}$ on the real axis in the complex- m plane that corresponds to the ATI threshold

$$m_{\text{th}} = \frac{\kappa^2}{2\omega} + \frac{U_p}{\omega} . \quad (4.1)$$

Transition to the cutoff region with N increasing corresponds to steep bending of the saddle point trajectory after which it moves almost perpendicular to the real axis. The reason of the trajectory bending is seen to be a “collision” with another saddle point shown by the circles in Fig. 3. In the “collision” region the two saddle points (“diamonds” and “circles”) abruptly change direction of motion forming the characteristic cross-like pattern. The “collision” occurs at $N = N_{\text{col}} \approx 35$. Approximately one can identify N_{col} with N_b . For $N < N_{\text{col}}$ the two saddle points m_c are to be taken into account in formula (3.8). As shown in Fig. 4, this improves the results for the rates in the plateau domain by producing appropriate structures in the N -dependence. Remarkably, such a two-saddle-point calculation gives correct positions of minima and maxima in the rate N -dependence, albeit the magnitudes of the rate variation is reproduced somewhat worse; for instance the depth of the minimum at $N = 17$ is quite strongly overestimated. Tentatively one can attribute this to the fact that if the principal term in the approximation for d_N^+ considered here proves to be anomalously

small for some N , then the correction terms omitted in our calculations become relatively important. The good overall description of the structure unambiguously identifies its nature as a result of an interference between the contributions coming from two effective ATI channels.

The plain saddle point approximation (3.8) presumes that the saddle points are well separated from each other; otherwise the more complicated uniform approximations are to be constructed. In our problem this refers to the “collision” region $N \approx N_{\text{col}}$ where our simple approximation somewhat overestimate rates; however we do not resort here to the more sophisticated mathematical constructions. Note that the third saddle point shown by triangles in Fig. 3 is substantial only in calculations for the lowest harmonics. Therefore it is not taken into account in the present calculations.

B. Scanning laser intensity for fixed harmonic order

It is equally instructive to see how the rate of some individual harmonic depends on the laser intensity I . Fig. 5 shows trajectories of the saddle points as I varies; only two most important saddle points are considered. For small intensities only the saddle point shown by diamonds is operative in evaluation of HG rate. This corresponds to the rapid-fall-off regime beyond the plateau domain. Here $\text{Im } m_c$ is large and negative. As I increases, the saddle point moves to the real m axis. After crossing the axis the trajectory abruptly bends at I about 3×10^{10} W/cm². For higher intensities, in the plateau domain, the second saddle point, shown by circles, should also be taken into account in calculation of HG rates. In this region the single-saddle-point approximation correctly reproduces an average behavior of the HG rate, whereas the two-saddle-point approximation shows also characteristic oscillations of the rate with I (Fig.6). The positions of minima and maxima are correctly reproduced for medium intensities. On the higher I side an additional maximum at $I = 9 \times 10^{10}$ W/cm² is beyond the two-saddle-point approximation being tentatively due to the contribution of the third saddle point omitted in the present calculations. This contribution could be also the source of an additional minor structure in the medium intensity region. It could explain also the fact that the two-saddle-point approximation gives deeper minima in the rates than the numerical summation in (1.1).

The present calculations clearly show that the structures in HG rates as function of I is related to the interference effects, in agreement with conclusion reached by Lewenstein *et al* [8]. The alternative explanation [10,11] relates this structure to the threshold effects, namely to the successive closure of ATI channels by increasing ponderomotive potential as I grows. However, the threshold effects should be manifested also in the single-saddle-point approximation; Fig. 6 demonstrates that this is not the case.

In the plateau regime the saddle point m_c shown by diamonds in Fig. 6 lies in the complex- m plane close to the threshold value m_{th} calculated for the same laser intensity using formula (4.1). As I increases, m_c tends to approach m_{th} . This behavior is in agreement with the three-step model developed by Corkum [3] who presumed that the ATI electron leaves an atom with zero velocity. Note however, that this presumption is valid only within single-saddle-point approximation (shown by diamonds in Fig. 5) and only in the plateau domain. The point $m = m_{\text{th}}$ is a branch point for any function which depends on m via K_m . In particular, generally the preexponential factor $\mathcal{Q}_{m\mu}$ (3.3) in expression (3.4)

has such a branch point. In principle one can look for some refined version of the saddle point approximation which accounts for closeness of a saddle point and a branch point. Note however that such modifications influence only the preexponential factor but not the exponent which is the principal object of interest. As discussed above, description of the transition between one-saddle point and two-saddle point regimes is more difficult for the semiclassical-type theory since it requires more sophisticated approach. In the present case the situation is aggravated by the presence of the branch point. It makes behavior of trajectories near the 'collision point' quite different from the conventional cross-like pattern (Fig. 5) and leads to appearance of a spike on the dashed curve in Fig. 6 at the borderline intensity $I = 2.7 \times 10^{10}$ W/cm².

V. CONCLUSION

The present study has an objective to get a better insight into the three-step mechanism of processes in strong laser field. We take HG as the simplest case of three-step process and employ representation of its amplitude in terms of amplitudes of physical, fully accomplished ATI and PLAR processes. The number of alternative paths in the three-step picture is generally infinite, each path being labeled by the number m of laser photons absorbed in the first step, ATI. We explore the range of substantial intermediate ATI channels and reveal crucial role of coherent interference. The effective scheme of summation of the contributions coming from different intermediate ATI channels is developed based on the saddle point method. Physically this approach is justified by the multiphoton nature of the process. Due to it in the strong-field regime both ATI and PLAR amplitudes have phases that vary rapidly with m . Within this framework we develop concept of effective ATI channels that is important basically and useful for practical calculations. In this approach interference of infinite number of competing paths is replaced by the single-path picture for generation of high harmonic, or by interference of two paths for harmonics lying in the plateau domain. In particular, the structure in HG rates in the latter domain is understood as the simple two-paths interference pattern.

The effective ATI channels are related to the particular classical electron trajectories that ensure that electron emitted from the atom at the first, ATI stage of HG process returns to the core to make possible subsequent laser assisted recombination. The possible trajectories possessing this property in principle comprise an infinite set differing by the excursion time in continuum which is integer multiple of laser period T . However due to quantum wave packet spread only the trajectories with the shortest excursion time provide substantial contribution to HG rate. The crucial step in this development is complexification of the problem: the initial and final time is complex-valued that makes entire classical trajectory also complex-valued. The simplicity of description achieved along these lines is in sharp contrast with the approach based on the conventional real-time classical trajectories where the problems related to chaotic irregular classical motion emerge in full scale [23].

ACKNOWLEDGMENTS

This work has been supported by the Australian Research Council. V. N. O. acknowledges the hospitality of the staff of the School of Physics of UNSW where this work has been carried out.

APPENDIX A: ATI AMPLITUDE IN ADIABATIC APPROXIMATION

The original expression for the ATI amplitude within the Keldysh [1] approximation reads

$$A_m(\mathbf{p}) = \frac{1}{T} \int_0^T dt' \langle \Phi_{\mathbf{p}}(t') | V_F(t) \hat{d}_{\epsilon} | \Phi_a(t') \rangle , \quad (\text{A1})$$

where $\Phi_{\mathbf{p}}$ is the Volkov state of the electron with the translational momentum \mathbf{p} , Φ_a is the electron initial bound state. Details of all the definitions could be found in Ref. [15]; here we indicate only that $V_F(\mathbf{r}, t) = \mathbf{r} \cdot \mathbf{F} \cos \omega t$ describes an interaction of the active electron and the laser field, with ω , \mathbf{F} and T being introduced in Sec. IB. The absolute value p_m of the electron momentum in the m -th ATI channel is subject to energy conservation constraint being given by formula (1.3) ($p_m = K_m$).

The adiabatic treatment of the ATI process was developed in Ref. [21] and subsequently applied in Refs. [22,14,15]. It presents the ATI amplitude $A_m(\mathbf{p})$ as

$$A_m^{(sp)}(\mathbf{p}) = \sum_{\mu} A_{m\mu}^{(sp)}(\mathbf{p}) , \quad (\text{A2})$$

$$A_{m\mu}^{(sp)}(\mathbf{p}) = -\frac{(2\pi)^2}{T} A_a \Gamma(1 + \nu/2) 2^{\nu/2} \kappa^{\nu} Y_{lm_{az}}(\hat{\mathbf{p}}) \frac{\exp[iS(t'_{m\mu})]}{\sqrt{-2\pi i S''(t'_{m\mu})^{\nu+1}}} , \quad (\text{A3})$$

where $S(t)$ is the classical action

$$S(t) = \frac{1}{2} \int^t d\tau \left(\mathbf{p} + \frac{\mathbf{F}}{\omega} \sin \omega \tau \right)^2 - E_a t . \quad (\text{A4})$$

The position of the saddle points $t'_{m\mu}$ in the complex t' plane is defined by equation

$$S'(t'_{m\mu}) = 0 , \quad (\text{A5})$$

or, more explicitly,

$$\left(\mathbf{p} + \frac{\mathbf{F}}{\omega} \sin \omega t'_{m\mu} \right)^2 + \kappa^2 = 0 . \quad (\text{A6})$$

Expression for HG amplitude (1.1) refers to the particular saddle point ($\mu = \mu_0$) defined for the monochromatic laser field by the expressions

$$\sin \omega t'_{m\mu_0} = \frac{\omega}{F} (-K_m + i\kappa) , \quad (\text{A7a})$$

$$\cos \omega t'_{m\mu_0} = \sqrt{1 - \frac{\omega^2}{F^2} (-K_m + i\kappa)^2} . \quad (\text{A7b})$$

The other notations are as follows: $\frac{1}{2}\kappa^2$ is initial electron binding energy, $\nu = Z/\kappa$, Z is the charge of the atomic residual core ($\nu = Z = 0$ for a negative ion), l , m_{az} are the active electron orbital momentum and its projection in the initial state. In the present context the unit vector $\hat{\mathbf{p}}$ coincides with $\hat{\mathbf{F}} = \mathbf{F}/F$. The coefficients A_a are specified in Ref. [21] being tabulated for many atoms and ions [24]. Mathematically formula (A2) is obtained by using the saddle point method to carry out integration over time variable t' in formula (A1). The saddle point positions are defined by Eqs. (A5) or (A6) that are to be considered together with the energy conservation constraint (1.3). The summation in (A2) runs over the saddle points $t'_{m\mu}$ in the plane of the complex-valued time t' . The saddle points $t'_{m\mu}$ lie symmetrically with respect to the real t' axis. For the monochromatic laser field there are four saddle points in the interval $0 \leq \text{Re } t'_{m\mu} \leq T$, two of them lying in the upper half plane ($\text{Im } t'_{m\mu} > 0$). Only these two saddle points are included into the summation in (A2). If ATI is considered as the first step in HG process, then, as discussed in detail in Ref. [15], only one of these two saddle points is effectively operative, namely, that specified by formulae (A7).

APPENDIX B: LAR AND PLAR AMPLITUDES IN ADIABATIC APPROXIMATION

The PLAR amplitude defined as

$$B_{N m\mu_0}(\mathbf{p}) = -\frac{1}{2\pi T} \int_0^T dt \frac{1}{R_0(t, t'_{m\mu_0})} \langle \Phi_a(t) | \exp(i\Omega t) \hat{d}_{\boldsymbol{\epsilon}} | \Phi_{\mathbf{p}}(t) \rangle , \quad (\text{B1})$$

differs from the LAR (Laser Assisted Recombination) amplitude $C_m(\mathbf{p})$

$$C_{Nm}(\mathbf{p}) = \frac{1}{2\pi T} \int_0^T dt \langle \Phi_{\mathbf{p}}(t) | \exp(i\Omega t) \hat{d}_{\boldsymbol{\epsilon}} | \Phi_a(t) \rangle \quad (\text{B2})$$

only by the ‘‘propagation’’ or ‘‘expansion’’ factor $1/[R_0(t, t'_{m\mu_0})]$ in the integrand. The distance passed by electron in the laser field between initial time t' and final time t is approximated as [15]

$$R_0(t, t') = \frac{F}{\omega^2} (\cos \omega t - \cos \omega t') . \quad (\text{B3})$$

In (B1), (B2) $\hat{d}_{\boldsymbol{\epsilon}} = \boldsymbol{\epsilon} \cdot \mathbf{r}$ is the dipole interaction operator.

Consider electron in the laser-dressed continuum state with the translational momentum \mathbf{p} . It can recombine to the bound state Φ_a with emission of the photon. Possible frequencies of the emitted photon Ω_j^{LAR} form an equidistant pattern:

$$\Omega_M^{\text{LAR}} = \frac{1}{2} \mathbf{p}^2 + U_p - E_a + M\omega \quad (\text{B4a})$$

with an integer M . Expression (B4a) can be reparametrized to the form

$$\Omega_j^{\text{LAR}} = (J + \eta)\omega, \quad (\text{B4b})$$

where J is another integer and the fractional parameter η ($0 \leq \eta < 1$) is governed by the value of the initial momentum p . In the zero-laser-field limit ($F \rightarrow 0$) only emission of the photon with the frequency $\Omega_{F \rightarrow 0}^{\text{LAR}} = \frac{1}{2} \mathbf{p}^2 - E_a$ is allowed. The presence of intensive laser field makes possible the processes when laser photons are absorbed from the field or transmitted to it, and thus the entire spectrum (B4) is produced. Such a LAR process has not yet received much attention in literature; as far as we know, our recent study [25] is the only theoretical paper on the subject. In it the initial electron translational momentum \mathbf{p} was considered as an arbitrary input parameter as required in applications to LAR process in laser plasma. In other terms, the fractional parameter η was arbitrary.

Here we are interested in LAR as a constituent part of HG process. This application has some particular features. First, all the frequencies in the photon spectrum are integer multiples of ω , i.e. $\eta = 0$. This happens because the initial translational momentum p of LAR process could not be arbitrary since only the discrete subset of continuum states is populated by ATI from the bound state. Namely, the translational momentum is subject to the constraint (1.3) with m being the number of laser photons absorbed on the initial ATI stage of HG process.

Second, when an individual harmonic is considered, its order N is fixed, and the parameter m is scanned when summation is carried out according to the expression (1.1a). Equivalently, the electron momentum $p = K_m$, is scanned along the discrete set of allowed values K_m , see Eq. (1.3). This is in variance with the laser plasma applications when it is natural to presume that \mathbf{p} is fixed and Ω^{LAR} is scanned. The third special feature is that the electron translational momentum $\mathbf{p} = \mathbf{K}_m$ is parallel to the electric field amplitude \mathbf{F} .

Finally, the object of interest in HG theory is the PLAR amplitude (B1) rather than LAR amplitude (B2), although both amplitudes are quite similar. Below we briefly expose modification of some results in the LAR theory relevant to the present application.

The expressions (B1) and (B2), respectively, for PLAR and LAR process amplitudes are valid in the Keldysh-type approximation. By using the Fourier transformation they are rewritten as

$$B_{Nm\mu_0}(\mathbf{K}_m) = -\frac{1}{2\pi T} \int_0^T dt \frac{1}{R_0(t, t'_{m\mu_0})} \exp\{i[\Omega t - S(t)]\} \tilde{\phi}_a^{(\epsilon)}\left(-\mathbf{K}_m - \frac{\mathbf{F}}{\omega} \sin \omega t\right), \quad (\text{B5})$$

$$C_{Nm}(\mathbf{K}_m) = -\frac{1}{2\pi T} \int_0^T dt \exp\{i[\Omega t - S(t)]\} \tilde{\phi}_a^{(\epsilon)}\left(-\mathbf{K}_m - \frac{\mathbf{F}}{\omega} \sin \omega t\right), \quad (\text{B6})$$

where the classical action $S(t)$ is introduced above by formula (A4). The function $\tilde{\phi}_a^{(\epsilon)}(\mathbf{q})$ is defined as

$$\tilde{\phi}_a^{(\epsilon)}(\mathbf{q}) = i(\boldsymbol{\epsilon} \cdot \nabla_{\mathbf{q}}) \tilde{\phi}_a(\mathbf{q}). \quad (\text{B7})$$

where $\tilde{\phi}_a(\mathbf{q})$ is the Fourier transform of the bound state wave function $\phi_a(\mathbf{r})$:

$$\tilde{\phi}_a(\mathbf{q}) = \int d^3\mathbf{r} \exp(-i\mathbf{q}\mathbf{r}) \phi_a(\mathbf{r}) . \quad (\text{B8})$$

The time integrals in (B5) and (B6) could be evaluated using the saddle point approximation:

$$B_{Nm\mu_0} = \frac{1}{2\pi T} \sum_{\mu} \frac{\omega^2}{F(\cos\omega t'_{m\mu_0} - \cos\omega t_{m\mu})} \tilde{\phi}_a^{(\epsilon)}\left(-\mathbf{K}_m - \frac{\mathbf{F}}{\omega} \sin\omega t_{m\mu}\right) \times \\ \times \sqrt{\frac{2\pi}{iS''(t_{m\mu})}} \exp\{i[N\omega t_{m\mu} - S(t_{m\mu})]\} . \quad (\text{B9})$$

$$C_{Nm} = -\frac{1}{2\pi T} \sum_{\mu} \tilde{\phi}_a^{(\epsilon)}\left(-\mathbf{K}_m - \frac{\mathbf{F}}{\omega} \sin\omega t_{m\mu}\right) \times \\ \times \sqrt{\frac{2\pi}{iS''(t_{m\mu})}} \exp\{i[N\omega t_{m\mu} - S(t_{m\mu})]\} , \quad (\text{B10})$$

where summation is to be taken over the saddle points $t_{m\mu}$ operative in the contour integration. The position of saddle points in the complex t -plane is governed by the equation

$$S'(t_{m\mu}) - \Omega = 0 , \quad (\text{B11})$$

or, more explicitly

$$\frac{1}{2} \left(\mathbf{p} + \frac{\mathbf{F}}{\omega} \sin\omega t_{m\mu} \right)^2 = E_a + \Omega . \quad (\text{B12})$$

Its solution is

$$\sin\omega t_{m\mu} = \frac{\omega}{F} \left(-K_m \pm \sqrt{2N\omega - \kappa^2} \right) . \quad (\text{B13})$$

For $N = 0$ the formula (B13) coincides with that governing the saddle point position in case of ATI processes [see Eq. (A7)]. As in the latter case, Eq. (B11) has four solution per the field cycle (i.e for $0 < \text{Re}t_{m\mu} < T$). Physically $t'_{m\mu_0}$ is the time when the electron is emitted at the first step of HG process and $t_{m\mu}$ is the time of electron return back to the initial bound state at the last stage. Note however that both $t'_{m\mu_0}$ and $t_{m\mu}$ are generally complex-valued.

Formula (B13) might give real-valued saddle points $t_{m\mu}$ that correspond to the classically allowed LAR or PLAR. According to Eq. (B12) this means emission of the high-energy photon at the real moments of time when the instantaneous kinetic energy of the electron in the laser field differs from the bound state energy E_a by Ω . In this respect LAR or PLAR processes differ basically from ATI process which is always described by the complex-valued saddle points that corresponds to the classically forbidden or tunneling transitions. The classically allowed transitions in LAR or PLAR are absent for small N when $N < \kappa^2/(2\omega)$. However we are interested only in generation of harmonics with sufficiently high order:

$$N > \frac{\kappa^2}{2\omega} . \quad (\text{B14})$$

In this case the classically allowed population is operative provided m is not too large, namely

$$K_m < \frac{F}{\omega} + \sqrt{2N\omega - \kappa^2} , \quad (\text{B15a})$$

i.e.

$$m < m_N^+ \equiv N + 3\frac{U_p}{\omega} + \frac{F}{\omega^2} \sqrt{2N\omega - \kappa^2} . \quad (\text{B15b})$$

If N is sufficiently large, namely if

$$\frac{F}{\omega} < \sqrt{2N\omega - \kappa^2} , \quad (\text{B16a})$$

i.e.

$$N > \frac{\kappa^2}{2\omega} + \frac{2U_p}{\omega} , \quad (\text{B16b})$$

then the domain of classically populated m -channels is bounded from below by the condition

$$K_m > -\frac{F}{\omega} + \sqrt{2N\omega - \kappa^2} , \quad (\text{B17a})$$

i.e.

$$m > m_N^- \equiv N + \frac{3U_p}{\omega} - \frac{F}{\omega^2} \sqrt{2N\omega - \kappa^2} . \quad (\text{B17b})$$

In the interval $m_N^- < m < m_N^+$ the classical population is governed by two real saddle points $t_{m\mu}$ per field cycle. Note that for the real LAR or PLAR process one always implies that the m -th ATI channel is open, i.e. m is sufficiently large:

$$m > m_{\text{th}} \quad (\text{B18})$$

where m_{th} is defined by Eq. (4.1). The same constraint is assumed also in the sum over m in formula (1.1a) implementing the three-step mechanism of HG [14,15].

For intermediate N lying in the interval

$$\frac{\kappa^2}{2\omega} < N < \frac{\kappa^2}{2\omega} + \frac{2U_p}{\omega} \quad (\text{B19})$$

another regime of classical population becomes possible. Namely, if the condition

$$K_m < \frac{F}{\omega} - \sqrt{2N\omega - \kappa^2} , \quad (\text{B20a})$$

i.e.

$$m_{\text{th}} < m < m_N^- \equiv N + \frac{3U_p}{\omega} - \frac{F}{\omega^2} \sqrt{2N\omega - \kappa^2} \quad (\text{B20b})$$

is satisfied, there are four saddle points $t_{m\mu}$ per field cycle.

In Fig. 7 we illustrate these results taking LAR of electron on hydrogen atom with formation of negative H^- ion. The laser field intensity is $I = 10^{11}$ W/cm². Open ATI channels lie at $m \geq 16$. The intermediate N regime (B19) takes place for $7 \leq N \leq 24$. In Fig. 7a we show m distributions of LAR modulus squared amplitudes $|C_{Nm}|^2$ for two adjacent N from the intermediate- N domain, $N = 13$ and $N = 15$. For $N = 13$ the classically forbidden domain is $m \geq 62$; the classical population in the two-saddle-point regime is operative for $19 \leq m \leq 61$, the four-saddle-point regime is operative for $16 \leq m \leq 18$. For $N = 15$ the classical population is forbidden for $m \geq 66$; it is allowed in the two-saddle-point regime for $18 \leq m \leq 66$; the four-saddle-point regime is operative for $16 \leq m \leq 17$. The region of transition from classically allowed to classically forbidden LAR requires some more elaborate treatment to reproduce related transition pattern similar to Airy function. The special analysis is required also to describe a transition from two-saddle-point to four-saddle point regime. However here we do not pursue the objective of detailed uniform description of LAR or PLAR amplitudes.

Note that for $N = 0$ the saddle points coincide with the singularity of the integrand $\tilde{\phi}_a^{(\epsilon)}(\mathbf{q})$. This coincidence occurs also in the adiabatic treatment of ATI. The difference is that in the particular case of above threshold detachment of negative ion the singularity in the integrand is canceled and the standard form of the saddle point approximation is applicable. Otherwise (i.e. in case of non-zero atomic core charge) the saddle point method is to be applied in the somewhat modified form. In case of LAR the singularity is always present, and hence the modified form of the saddle point method should be applied for $N = 0$. Respectively, the small N case requires some special treatment (some sort of uniform approximation; note that all these modifications affect only the pre-exponential factor, but the principal exponent remains the same). Below we are interested in the large N case that allows us to put aside these complications. However, it is to be remembered that coincidence of the saddle point and the singularity of the momentum space wave function means that only large- r asymptote of the initial state wave function $\varphi_a(\mathbf{r})$ in the coordinate space is of importance. This is the case for ATI, but not for LAR or PLAR, as follows from the preceding discussion. In other words, the LAR amplitude (or its PLAR counterpart) generally are more sensitive for the short-range behavior of the wave function.

REFERENCES

- * Permanent address: Institute of Physics, The University of St Petersburg, 198904 St Petersburg, Russia.
- [1] L. V. Keldysh, Zh. Eksp. Teor. Fiz. **47**, 1945 (1964) [Sov. Phys.-JETP **20**, 1307 (1965)].
- [2] M. Yu. Kuchiev, Pis'ma Zh. Eksp. Teor. Fiz. **45**, 319 (1987) [JETP Letters **45**, 404 (1987)].
- [3] P. B. Corkum, Phys. Rev. Lett. **71**, 1994 (1993).
- [4] J. L. Krause, K. J. Schafer, and K. C. Kulander, Phys. Rev. Lett. **68**, 3535 (1992).
- [5] K. C. Kulander, K. J. Schafer, and J. L. Krause, in *Super-Intense Laser-Atom Physics*, Vol.316 of *NATO Advanced Study Institute, Series B: Physics*, edited by B. Piraux et al (Plenum, New York, 1993), p. 95.
- [6] A. L'Huillier, M. Lewenstein, P. Sallièrs, Ph. Balcou, M. Yu. Ivanov, J. Larsson, and C. G. Wahlström, Phys. Rev. A **48**, R3433 (1993).
- [7] M. Lewenstein, Ph. Balcou, M. Yu. Ivanov, A. L'Huillier, and P. B. Corkum, Phys. Rev. A **49**, 2117 (1994).
- [8] M. Lewenstein, P. Sallièrs, and A. L'Huillier, Phys. Rev. A **52**, 4747 (1995).
- [9] W. Becker, S. Long, and J. K. McIver, Phys. Rev. Lett. **41**, 4112 (1990).
- [10] W. Becker, S. Long, and J. K. McIver, Phys. Rev. A **46**, R5334 (1992).
- [11] W. Becker, S. Long, and J. K. McIver, Phys. Rev. A **50**, 1540 (1994).
- [12] M. Yu. Kuchiev, J. Phys. B **28**, 5093 (1995).
- [13] M. Yu. Kuchiev, Phys. Lett. A **212**, 77 (1996).
- [14] M. Yu. Kuchiev and V. N. Ostrovsky, J. Phys. B **32**, L189 (1999).
- [15] M. Yu. Kuchiev and V. N. Ostrovsky, Phys. Rev. A **60**, 3111 (1999).
- [16] A. Becker and H. F. M. Faisal, J. Phys. B **29**, L197 (1996).
- [17] H. F. M. Faisal and A. Becker, Laser Physics **7**, 684 (1997); A. Becker and H. F. M. Faisal, Laser Physics **8**, 69 (1998).
- [18] A. Becker and H. F. M. Faisal, Phys. Rev. A **59**, R1742 (1999).
- [19] L. D. Landau and E. M. Lifshitz, *Quantum Mechanics* (Pergamon Press, Oxford, 1965); P. D. B. Collins, *An Introduction to Regge Theory & High Energy Physics* (Cambridge University Press, Cambridge, 1977).
- [20] In the detailed picture [21] an electron emerges from the under barrier at the source point separated from the core. There are two such points lying up and down the electric field vector in the laser wave. The related contributions interfere giving raise to the oscillatory patterns in the ATI angular distributions. These physically essential features of HG mechanism are not manifested in the saddle point equation (3.15) governing the momentum K_{m_c} : this equation does not distinguish between position in space of the source points and the atomic core.
- [21] G. F. Gribakin and M. Yu. Kuchiev, Phys. Rev. A **55**, 3760 (1997); J. Phys. B **30**, L657 (1997).
- [22] M. Yu. Kuchiev and V. N. Ostrovsky, J. Phys. B **31**, 2525 (1998); Phys. Rev. A **59**, 2844 (1999).
- [23] G. van de Sand and J. M. Rost, Phys. Rev. Lett. **83**, 524 (1999).
- [24] A. A. Radzig and B. M. Smirnov, *Reference Data on Atoms, Molecules and Ions* (Berlin: Springer, 1985).

- [25] M. Yu. Kuchiev and V. N. Ostrovsky, Phys. Rev. A **61**, 033414 (2000). Note that this paper employed definition of LAR amplitude as 2π times expression (B2).

FIGURES

FIG. 1. Contributions to the HG amplitude d_N^+ from different ATI m -channels according to the expression (1.1). The H^- ion in the laser field with the frequency $\omega = 0.0043$ and intensity $I = 10^{11}$ W/cm² produces harmonic of the order N indicated in the plots. The square moduli $|M_m|^2$ and phases $\arg(M_m)$ of three different amplitudes M_m are pictured. The closed circles show the squared moduli and phases of the terms $d_{Nm}^+ \equiv A_{m\mu_0} B_{Nm\mu_0}$ in the sum (1.1) over ATI channel label m . We present also the squared moduli and phases of the physically meaningful factors that constitute d_{Nm}^+ : ATI amplitude $A_{m\mu_0}$ (open squares) and PLAR amplitude $B_{Nm\mu_0}$ (open triangles). For graphical representation the convenient scaling factors are introduced in the plots of squared moduli, namely as $|M_m|^2$ we show everywhere $10^8 |2d_{Nm}^+|^2$, and also: for $N = 15 - 10^6 |A_{m\mu_0}|^2$ and $10^4 |B_{Nm\mu_0}|^2$; for $N = 25 - 5 \cdot 10^4 |A_{m\mu_0}|^2$ and $10^4 |B_{Nm\mu_0}|^2$; for $N = 39 - 10^4 |A_{m\mu_0}|^2$ and $10^4 |B_{Nm\mu_0}|^2$; for $N = 51 - 3 \cdot 10^3 |A_{m\mu_0}|^2$ and $10^4 |B_{Nm\mu_0}|^2$.

FIG. 2. The universal function $f(\xi)$ (3.27).

FIG. 3. Trajectories of the saddle points $m_c(N)$ in the complex- m plane for fixed laser intensity $I = 10^{11}$ W/cm² and varying harmonic order N . The results are for H^- ion in the laser field with the frequency $\omega = 0.0043$. Positions of three saddle points for odd integer N are denoted respectively by diamonds, circles and triangles. The plot (a) gives general overview, the plot (b) shows the region where two saddle points “collide”, whereas the plot (c) details behavior of the saddle point trajectory in the vicinity of $m = m_{th}$.

FIG. 4. Harmonic generation rates (1.4) (in sec^{-1}) for H^- ion in the laser field with the frequency $\omega = 0.0043$ and various values of intensity I as indicated in the plots. Closed circles - results obtained by Becker *et al* [11], open circles - our calculations [15] in the dipole-length gauge performing numerical summation (1.1) over contributions of different ATI channels, open diamonds - present results within the saddle point approximation (3.8) for the summation over ATI channels contributions with a single saddle point $m_c(N)$ taken into account (namely, the saddle point shown by diamonds in Fig. 3); open squares - same but taking into account two saddle points $m_c(N)$ (namely, these shown by diamonds and circles in Fig. 3).

FIG. 5. Trajectories of the saddle points $m_c(N)$ in the complex- m plane for fixed harmonic order $N = 15$ and varying laser intensity $I = \zeta \times 10^{10}$ W/cm² (HG by H^- ion in the laser field with the frequency $\omega = 0.0043$ is considered as in Fig. 3). The plot (a) gives general overview, the plot (b) shows vicinity of the real- m axis. Positions of two saddle points for odd integer N are denoted respectively by diamonds and circles with the numbers indicating value of the factor ζ , i.e. intensity in the units 10^{10} W/cm². The crosses in the plot (b) show positions of the ATI threshold defined by formula (4.1) for the same values of ζ .

FIG. 6. The rate parameter $M_N \equiv 2 \log_{10} |d_N^+|$ for the harmonic $N = 15$ as a function of the laser field intensity I (HG by H^- ion in the laser field with the frequency $\omega = 0.0043$). Solid curve - our calculations [15] in the dipole-length gauge performing numerical summation (1.1) over contributions of different ATI channels, dashed curve - present results within the saddle point approximation (3.8) for the summation over ATI channels contributions with a single saddle point $m_c(N)$ taken into account (namely, the saddle point shown by diamonds in Fig. 5); dotted curve - same but taking into account two saddle points $m_c(N)$ (namely, these shown by diamonds and circles in Fig. 3). The bars with numbers m indicate the threshold intensities I_m such that for $I > I_m$ the m -th ATI channel is closed due to ponderomotive potential.

FIG. 7. Squared modulus of the amplitude C_{Nm} of the laser assisted recombination of electron into H^- bound state in the laser field with the frequency $\omega = 0.0043$ and intensity $I = 10^{11}$ W/cm². The harmonic order is fixed [$N = 13$ (circles) and $N = 15$ (triangles) in (a) and $N = 39$ (circles) in (b)]. Closed symbols - calculations using the formula (B6) with numerical integration over t ; open symbols - adiabatic approximation (B10) with various number of saddle points taken into account for different m as described in the text.

Fig. 1, part 1

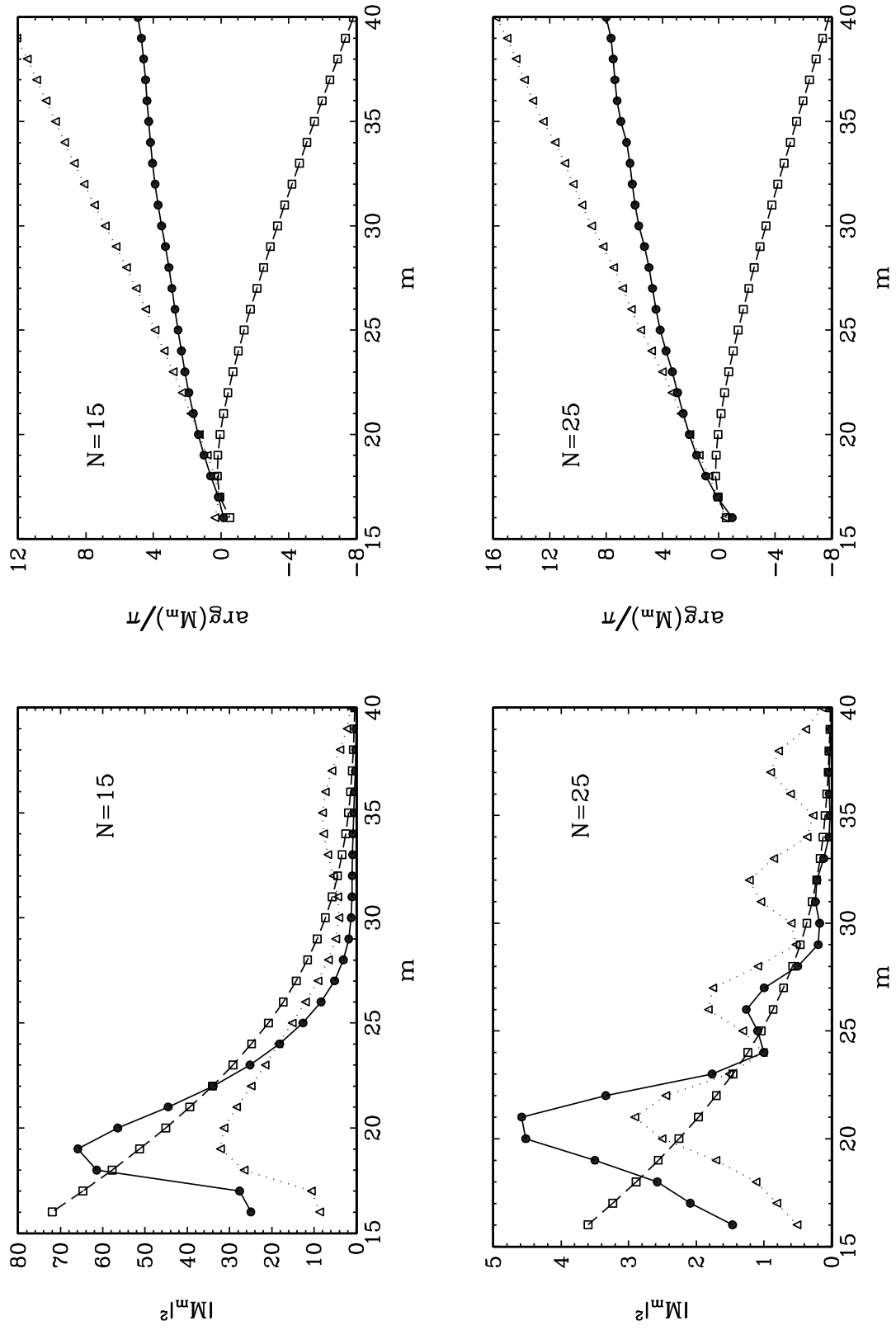


Fig. 1, part 2

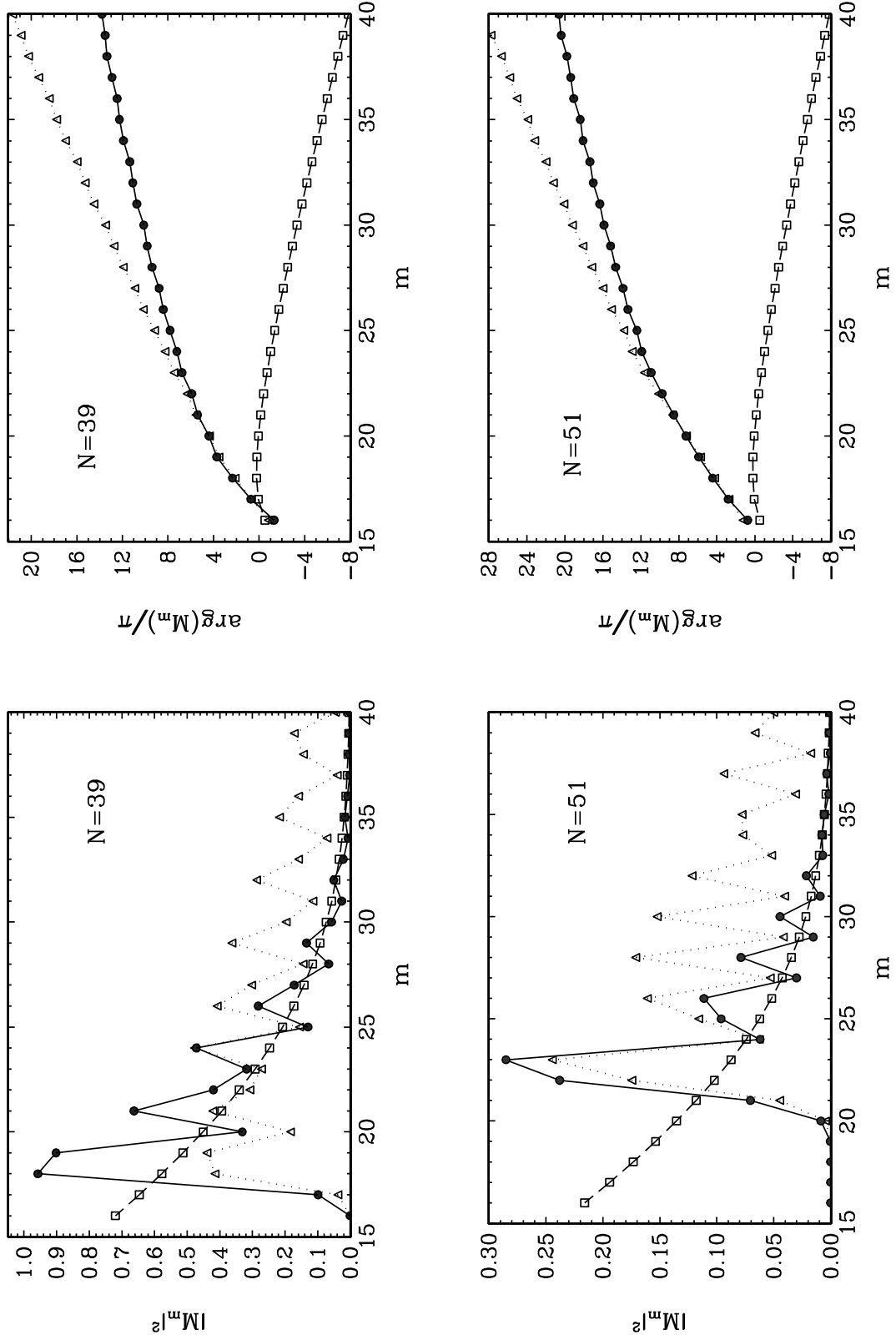


Fig. 2

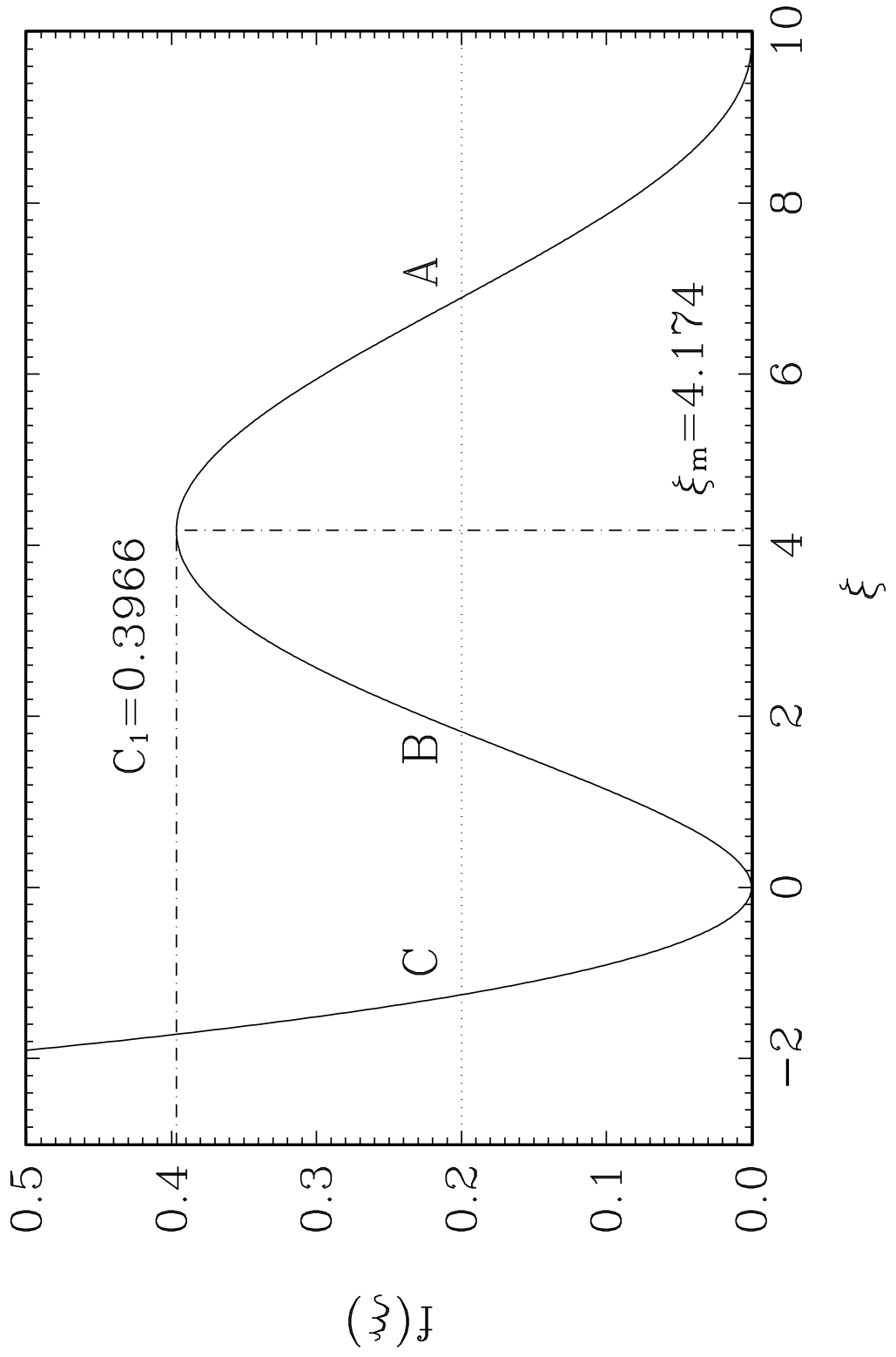
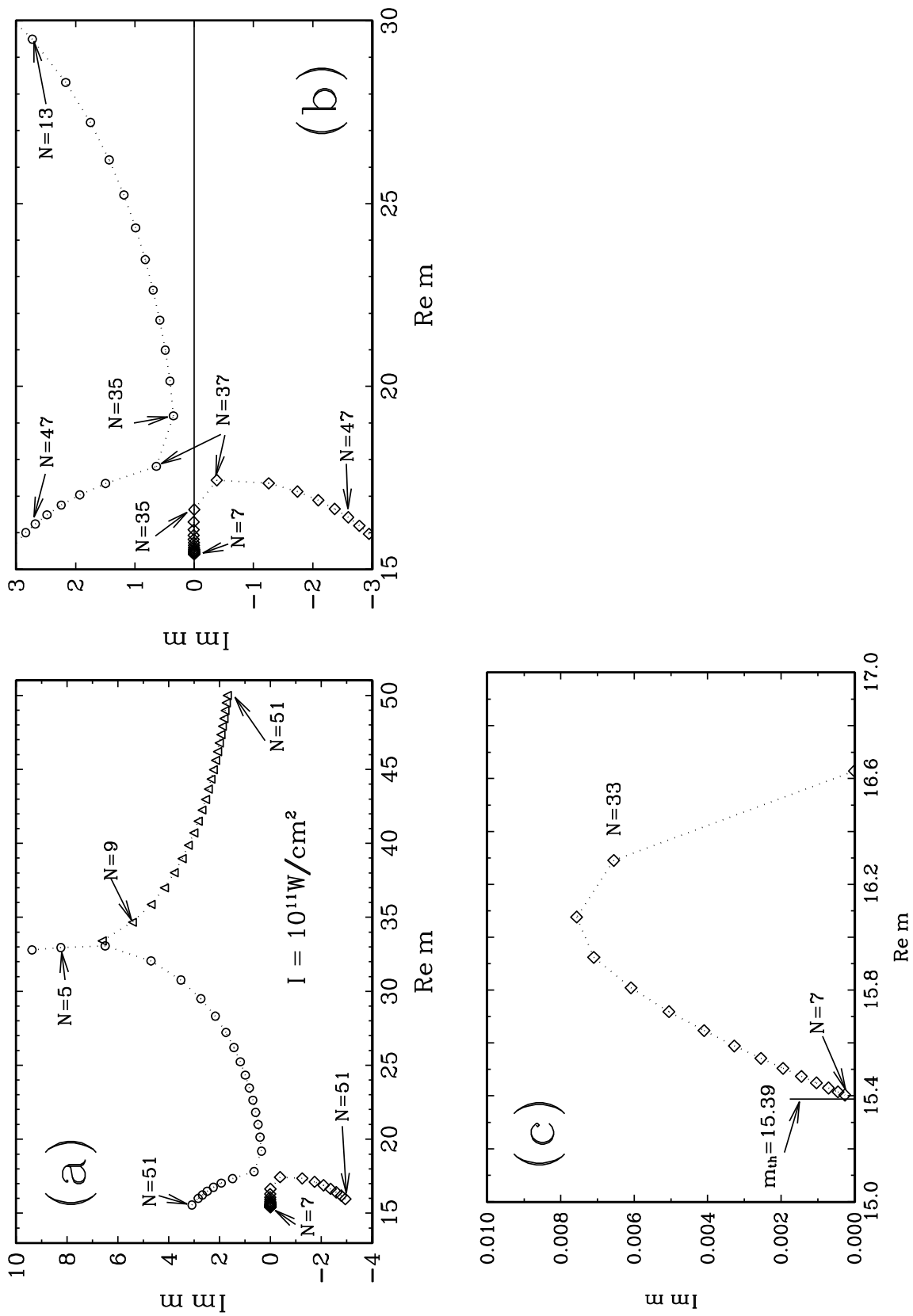


Fig. 3



HSUMHG

Fig. 4

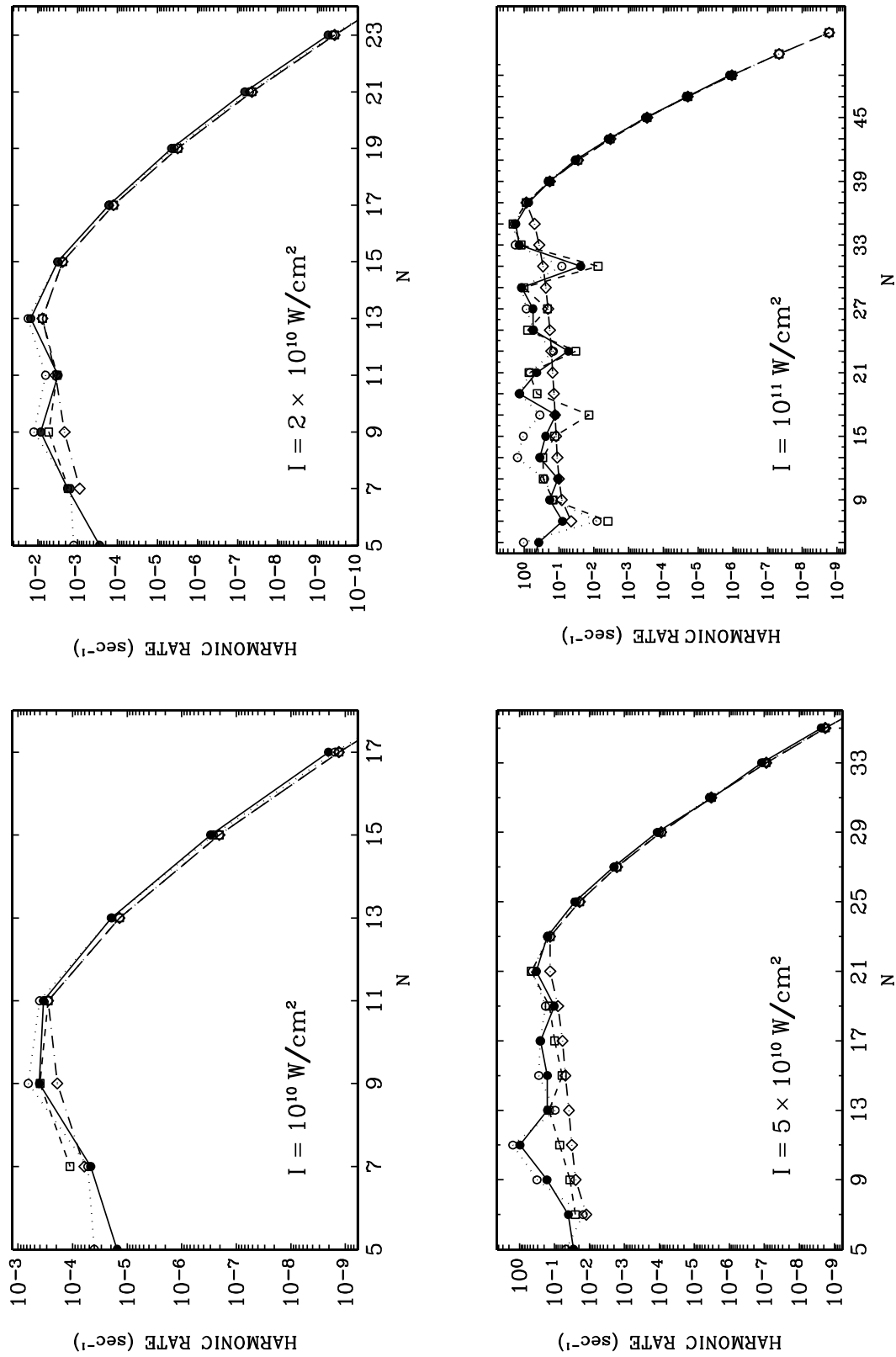


Fig. 5

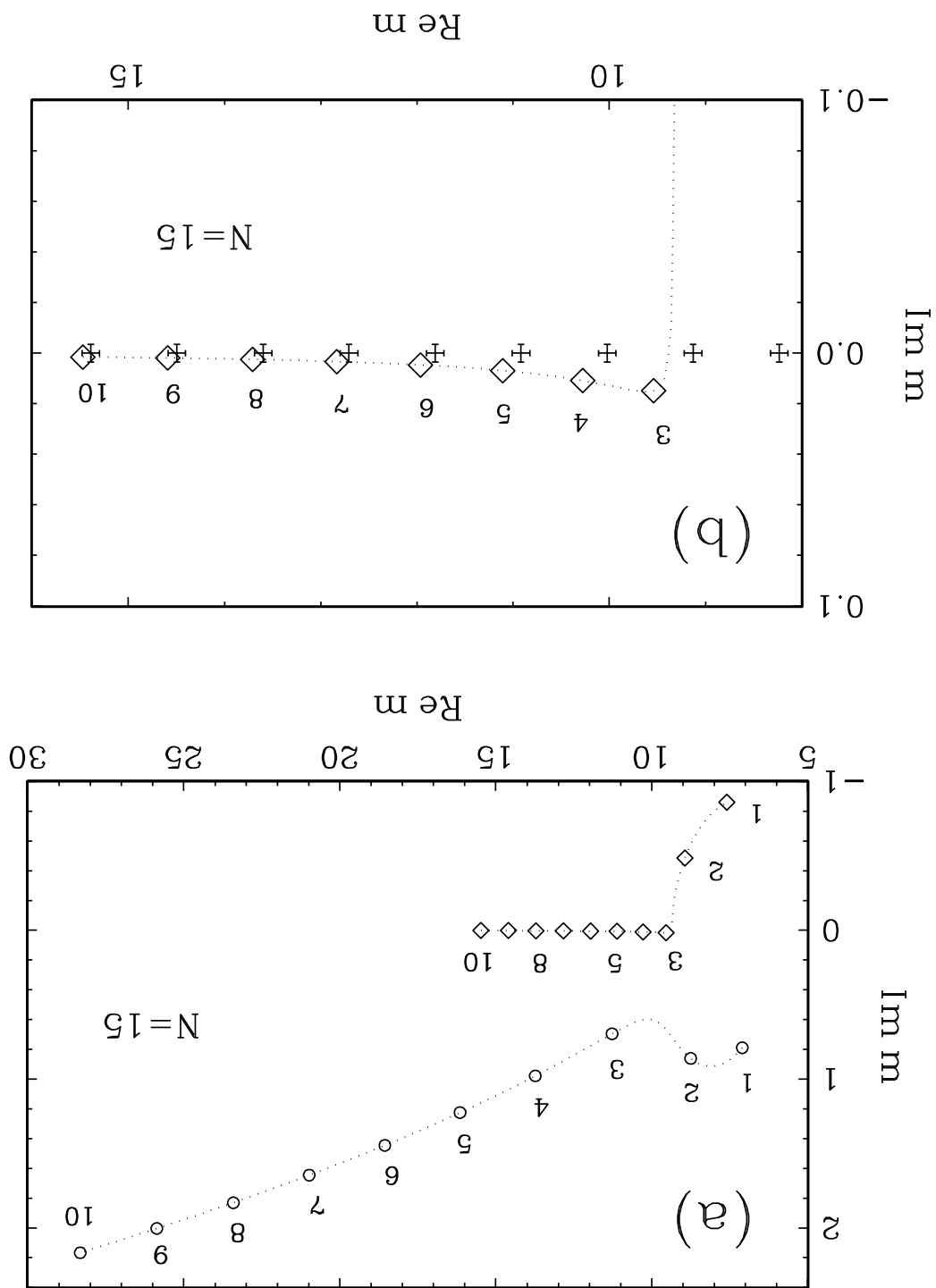


Fig. 6

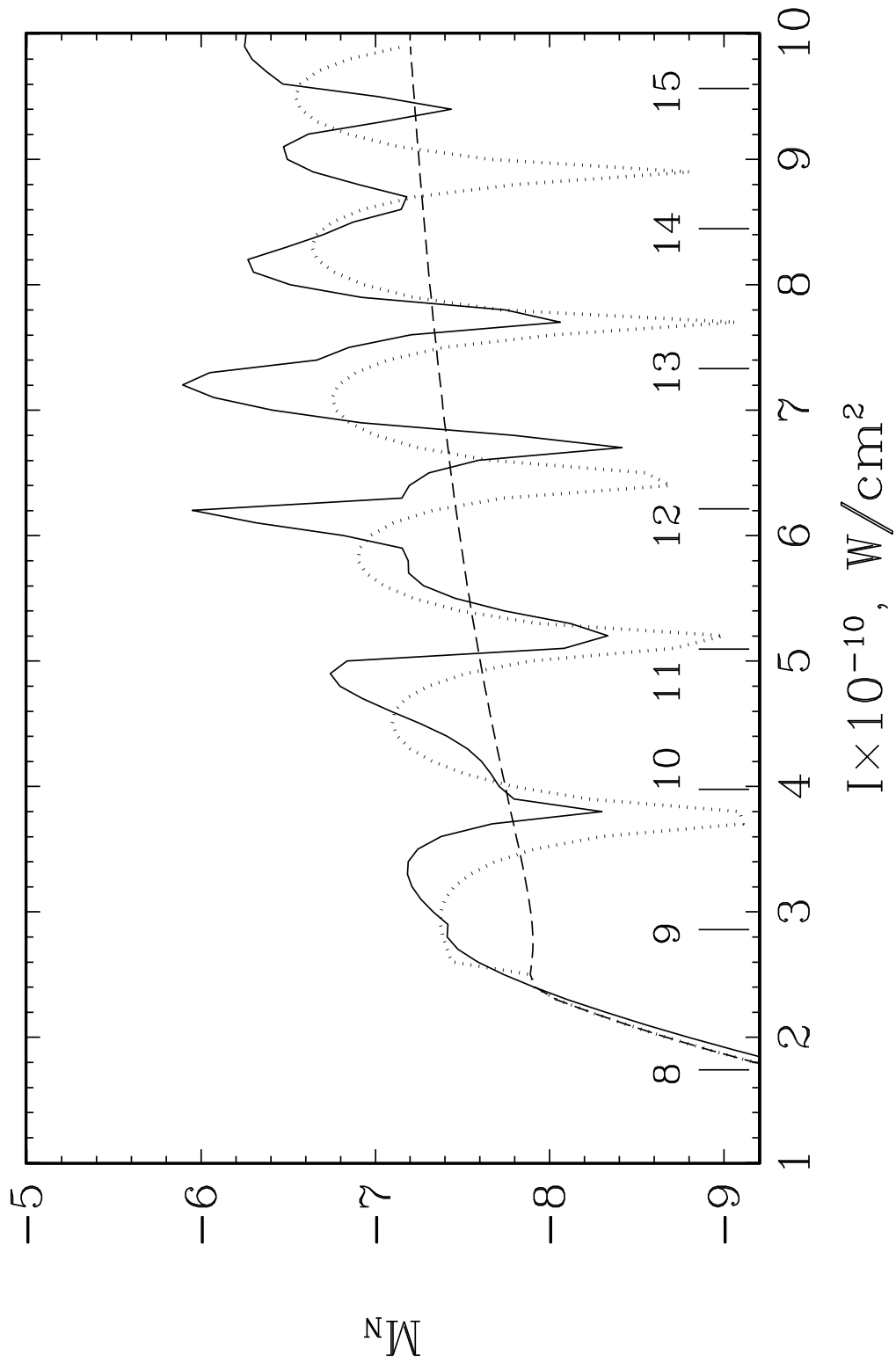


Fig. 7

